



## **CHAPTER 1**

### **Introduction**

<b>1.1 Importance of the present work</b>	<b>2</b>
<b>1.2 Basic concept of Neutron-induced reaction</b>	<b>5</b>
<b>1.2.1 Neutron-induced fission reaction</b>	<b>6</b>
<b>1.2.1.1 Fission Barrier</b>	<b>7</b>
<b>1.2.1.2 Brief overview of Fission Theory</b>	<b>7</b>
<b>1.2.1.3 Types of Fission Yields</b>	<b>11</b>
<b>1.2.2 Neutron Activation method – A tool for Neutron Cross-section Measurement</b>	<b>14</b>
<b>1.2.2.1 Principle of Neutron Activation Analysis</b>	<b>14</b>
<b>1.2.2.2 Kinetics of activation</b>	<b>14</b>
<b>1.2.2.3 Advantages and Limitations of NAA</b>	<b>15</b>
<b>1.2.3 Role of Structural materials in reactor technology</b>	<b>16</b>
<b>1.3 Various types of neutron sources</b>	<b>16</b>
<b>1.3.1 Neutrons from uranium fission - Nuclear Reactors</b>	<b>16</b>
<b>1.3.2 Radioactive (<math>\alpha</math>, n) sources</b>	<b>17</b>
<b>1.3.3 Accelerated charged particle based neutron sources</b>	<b>18</b>
<b>1.3.4 Photo-neutron sources</b>	<b>19</b>
<b>1.4 Solid State Nuclear Track Detector (SSNTD)</b>	<b>19</b>
<b>1.4.1 An application of solid state nuclear track detector in nuclear fission</b>	<b>20</b>
<b>1.5 A detailed literature survey related to the present work</b>	<b>21</b>
<b>1.6 Objective of the present thesis</b>	<b>23</b>
<b>1.7 Content of the present thesis</b>	<b>24</b>
<b>References</b>	<b>26</b>

### 1.1 Importance of the present work

Energy is a vital element of sustainable development. Large-scale growth in energy with need to control green house gas emissions has necessitated emphasis on nuclear power, a viable source of energy [1]. The widespread growth of nuclear energy has to address concerns relevant to proliferation risks also. It appears that hesitations in further developments of nuclear power are primarily due to the governmental concerns arising from the nuclear waste disposal schemes involving long-term geological storage of commercial reactor waste. For future growth of nuclear power, it will be necessary to satisfactorily address the troublesome issue of disposal of the nuclear waste, in particular long-lived transuranic elements (TRU), e.g.  $^{237}\text{Np}$ ,  $^{240}\text{Pu}$ ,  $^{241}\text{Am}$ ,  $^{243}\text{Am}$ ,  $^{244}\text{Cm}$  etc. and fission products (FP), e.g.  $^{129}\text{I}$ ,  $^{135}\text{Cs}$ ,  $^{99}\text{Tc}$ ,  $^{93}\text{Zr}$ ,  $^{107}\text{Pd}$  etc. The nuclear waste disposal is certainly an urgent and important issue to be tackled to ensure future growth of nuclear power. The fuel cycle based on thorium can address both these issues owing to a number of favorable neutronics and material characteristics which makes thorium a better fertile host [2]. The  $^{232}\text{Th}$ - $^{233}\text{U}$  fuel cycle has an advantage over the present reactor based on uranium fuel from the point of thousand times less radiotoxic waste production. Further, Thorium in its natural form consist almost all of  $^{232}\text{Th}$  with some trace amounts of  $^{230}\text{Th}$ . Its half life is more than that of  $^{238}\text{U}$ , therefore its occurrence on the earth's crust is nearly three times as that of uranium. Thus, Thorium is an attractive fuel option for contributing to large-scale global deployment of nuclear energy to meet rising demands [2].

Thorium is a fertile material and has to be converted into  $^{233}\text{U}$ , a fissile isotope. The cross-section for capture of thermal neutrons in  $^{232}\text{Th}$  is typically 2.47 times that in  $^{238}\text{U}$ . Thus thorium offers greater competition to capture of the neutrons and lower losses to structural and other parasitic materials leading to an improvement in conversion of  $^{232}\text{Th}$  to  $^{233}\text{U}$ . In addition, of the three fissile species ( $^{233}\text{U}$ ,  $^{235}\text{U}$  and  $^{239}\text{Pu}$ ),  $^{233}\text{U}$  has the highest value of 'η' value (number of neutrons released per neutron absorbed) that remains nearly constant over a wide energy range, in thermal as well as epithermal regions, unlike  $^{235}\text{U}$  and  $^{239}\text{Pu}$ . This facilitates achievement of high conversion ratios with thorium utilization in reactors operating in the thermal/epithermal spectrum. Further, thorium has important physical characteristics. The thermal conductivity of  $\text{ThO}_2$  is higher than that of  $\text{UO}_2$  fuel, leading to reduced fission gas release. The fission product

release rates for  $\text{ThO}_2$  based fuels are one order of magnitude lower than that of  $\text{UO}_2$ .  $\text{ThO}_2$  has a very high melting point of  $3300^\circ\text{C}$ .

India has vast resources of thorium in the country for nuclear power generation. Considering the large thorium reserves in country, the future nuclear power program will be based on  $^{232}\text{Th}$ - $^{233}\text{U}$  fuel cycle [3, 4]. By considering the above fact, it has been realized that there is a strong need for the development of thorium based technologies for the entire fuel cycle. The Advanced Heavy Water Reactor (AHWR) has been designed to fulfill this need and maximum power generation from thorium in India [4]. The brief detail of AHWR has been given in chapter 2. On the other hand, Bowman [5] and C. Rubbia et al [6] have proposed the concept of Accelerator-Driven Sub-critical reactor Systems (ADS) which demonstrate that a commercial nuclear power plant of adequate power can also be built around a sub-critical reactor, provided it can be fed externally with required intensity of accelerator-produced neutrons. The ADS have attractive features for the elimination of troublesome long-lived minor actinides and fission products of the spent fuel, as well as for nuclear energy generation utilizing thorium as fuel. In Europe, USA and Japan, the current interest in the ADS – also called hybrid reactor system- has been largely stimulated by the fact that a sub-critical core is ideally suited to safely incinerate the long-lived transuranics and fission products, which constitute the troublesome component of nuclear waste for disposal in deep geological repository. In ADS, high energy proton beam (around 1 GeV) strikes a heavy element target like W, Pb or Bi target, which yields copious neutrons by (p, xn) spallation reaction. Therefore, the spallation target becomes a source of neutrons, which can achieve self-terminating fission chain in a sub-critical core. In general, each energetic proton can yield 20-30 neutrons at proton energies around 1 GeV in high Z target materials.

For India, which has abundant reserves of thorium, ADS is relevant because one can also exploit its potential to design hybrid reactor systems that can produce nuclear power with the use of thorium as the main fuel [3]. The ADS based thorium burners may need only small and limited quantities of uranium and plutonium to serve as starter seeds. In general, the additional degree of freedom provided by the external source in ADS can enable one to design reactor systems which primarily burn thorium fuel as well as make a more efficient use of the uranium

fuel. Therefore, ADS seems to have the potential to provide an additional route an efficient and economic nuclear power generation with the available thorium resources. The overview of the ADS system from the point of view of the India's perspective has been given elsewhere [3]. A brief detail of ADS has been covered in chapter 2 of this thesis.

The development of ADS systems and Indian advanced reactor programme [4, 7-8] requires significant amount of new and improved nuclear data [9] in extended energy regions as well as for a variety of new materials. The importance of nuclear data needs at the very beginning of the evolution of the concept of energy amplifier (EA) has also been recognized by C. Rubbia [5]. In ADS, the actual conversion of fertile to fissile nuclei (e. g.  $^{232}\text{Th}$  to  $^{233}\text{U}$ ) or the transmutation of radioactive nuclei to stable ones takes place in blanket favorably in the resonance energy region and thermal regions where the capture cross-section is the largest. Thus, nuclear data to predict nuclear collision, isotope production, formation of gases and heat generation are needed at this very first step. Further, the energy produced in ADS or any nuclear reactor is due to neutron-induced fission of actinides. Therefore for the design of ADS, it is necessary to have accurate knowledge of nuclear data of actinides such as yields of fission products, neutron capture cross-sections and decay data including half-lives, decay energies, branching ratios etc. A major application fission product yields measurements is to determine the nuclear fuel burn up. In particular, the cumulative yields of short-lived fission products and independent yields of various fission products are important for the decay heat calculations. The reliability of fuel burn up is directly proportion to reliability of fission products yield values. Besides, the fission products yields are needed for mass and charge distribution studies to test the  $Z_p/A_p$  model used for prediction of unmeasured yields. Such studies can provide information about understanding of the process of nuclear fission. In addition, nuclear data are also needed to reduce the risk related to radiological release or other detrimental consequences. Nuclear data for (p, xn), (p, xp), (n, xn) and (n, xp) reactions are needed as a function of incident energy and ejectiles emitted at various emission angle and energies for all materials directly exposed to the particle beam. Further, for shielding calculations, (p, x $\gamma$ ), (n, x $\gamma$ ) and (n, xn) yield data are needed. Nuclear data for the calculation of displacement damage cross-sections with hydrogen and helium production cross-section up to high energies for structural materials (e. g, Zr, Ni, Fe, Al) are required. The Indian nuclear data activities for ADS have been discussed earlier in quite

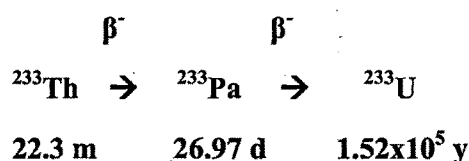
detail [9]. The nuclear data of isotopes of thorium fuel cycle have not been paid enough attention in the past, until 2000 [10]. Nuclear data of minor actinides and fission products are also crucial in international formulation of radioactive transport regulations. These requirements demonstrate the immediate need for experimental research, the result of which would be incorporated with the basic nuclear data. The generation and use of nuclear data are considered fundamentally important, as accurate nuclear data are essential inputs to simulate nuclear interactions to obtain the engineering parameters. Nuclear power is an inevitable option for India. India has national policy to implement a closed fuel cycle programme involving multiple fuels [11].

## 1.2 Basic concept of Neutron-induced reactions

Neutron-induced reactions are a special class by themselves. Since neutrons do not have charge, there is no coulomb barrier for neutron interaction with the nucleus. Therefore, neutrons of any energy can induce reactions with all the nuclides in the nuclide chart. The zero energy neutrons can produce exoergic reactions. For endoergic reactions, the incident neutrons must have kinetic energy greater than the reaction threshold.

The (n,γ) reactions have positive Q value. Another interesting aspect is that the reaction cross-sections with low energy neutrons are much larger compared to those by medium and high energy neutron-induced reactions. Nuclear reactor is a vast source of neutrons of different energy. There are other reactions which produce neutrons of definite energy which can be used as projectiles. The details of different types of neutron sources have been given in section 1.3 of this chapter. Neutron-induced reaction lead to the production of different ejectiles of the type (n, p), (n,α) etc, or simply to production of radioisotopes by (n,γ) reactions.

An important nuclide  $^{233}\text{U}$  for energy production is produced by neutron irradiation of  $^{232}\text{Th}$  followed by two successive  $\beta$  decays as shown below.



Neutron-induced reactions are important for a wide range of applications in field of Astrophysics, National security, Reactors etc. It is important to accurately predict a wide range

of processes that can occur with neutron energies ranging from eV to 10-20 MeV, inelastic scattering -direct, compound, and pre-equilibrium and also fission reactions. The measured neutron-induced reaction cross-section is required with the accuracy of 1 – 20 %. The above mentioned accuracy range of the neutron cross-section depends upon the particular application.

### 1.2.1 Neutron-induced fission reaction

In nuclear fission, a heavy nucleus like  $^{235}\text{U}$ , when bombarded with neutrons, undergoes division releasing a large amount of energy of about 200 MeV. This process is also accompanied by the emission of 2 to 3 neutrons which makes it possible to have a chain reaction for sustained production of energy. In the complete fission of 1 gram of  $^{235}\text{U}$ ,  $8.2 \times 10^{17}$  ergs of energy release, which is equal to 1 MW of power production per day. To obtain the same amount of energy, 3 tons of coal or 2300L of petrol has to be combusted. This shows that nuclear is more than million times energy intense compared to chemical energy [12].

Various stages of the fission process starting from compound nucleus (CN) formation to the formation of fission products are depicted in Fig. 1.1. A heavy nucleus of mass  $A > 200$  such as uranium forms a compound nucleus after absorbing a neutron and acquires certain excitation energy ( $E^*$ ). The compound nucleus deexcites by (i) emission of prompt gamma rays to its ground state, or (ii) undergoes  $\beta$  decay and forms an element of higher charge or (iii) undergoes  $\alpha$  decay and forms an element of lower charge and mass or (iv) undergoes nuclear fission. The compound nucleus having excitation energy undergoes continuous deformation mode. While the nucleus deforms, the repulsive coulomb energy and attractive surface energy change continuously. When the disruptive coulomb forces overcome attractive forces to surface energy, the nucleus undergoes division into two fragments. They move in opposite directions due to mutual coulomb repulsion which ultimately reflects in their kinetic energy. The fragments are formed in excited state and emit neutrons and gamma rays. The resulting products have higher N/Z ratio compared to stable nuclei undergo  $\beta$  decay to attain stability with stable end products.

In neutron-induced fission of  $^{235}\text{U}$ , about 200MeV of energy is liberated as mentioned in the beginning of this section 1.2.1. It can be calculated from the average binding energy of the fissioning nucleus and products. The compound nucleus  $^{236}\text{U}^*$  has an average binding energy

(B/A) of 7.6 MeV. Thus the total binding energy of  $^{236}\text{U}$  is equal to  $7.6 \times 236 = 1793.6$  MeV. Similarly the products have B/A around 8.5 MeV. Assuming that the average mass of fission products is around 120, total binding energy of both fragments is equal to  $236 \times 8.5 = 2006$  MeV, which is greater than the binding energy of  $^{236}\text{U}$ . The difference, equal to 214.4 MeV, is liberated in fission process. This is an approximate estimate as exact values of B/A for each fragment is not taken. The most direct method is to calculate the mass difference before and after the fission reaction for a given mass division. The mass division in nuclear fission is not unique. Therefore, the products need not be same for each fissioning atom of  $^{235}\text{U}$ .

### 1.2.1.1 Fission Barrier

Minimum energy required for a nucleus to undergo fission is called fission barrier. It is somewhat similar to activation energy in a chemical reaction wherein an activated intermediate is formed which might lead to the formation of products in the chemical reaction. In the case of nuclear fission, a fissioning nucleus has to attain critical shape, similar to a saddle, for the nucleus to undergo fission. This intermediate structure has more potential energy (PE) compared to the PE of the nucleus in ground state. The difference between these two PE's is called fission barrier. If the  $E^*$  of the CN exceeds the fission barrier, then fission reaction can take place. e.g., fission barrier of  $^{235}\text{U}$  is 5.6 MeV. After absorbing a thermal neutron it forms a CN  $^{236}\text{U}$  with an excitation energy of 6.5 MeV. Therefore,  $^{235}\text{U}$  is a fissionable with thermal neutrons. Nuclides which undergo fission with neutrons of all energies, including thermal neutrons are called fissile nuclides. It can be shown that this barrier height depends on  $Z^2/A$  of fissioning nucleus. The larger the value of  $Z^2/A$ , lesser is the barrier height. Experimentally fission barriers are determined for a large variety of actinide nuclides. One of the methods is to use photons of different energies and measure the fission product activity so as to locate fission threshold.

### 1.2.1.2 Brief overview of Fission Theory

Meitner and Frisch explained the fission process using the liquid drop model (LDM) of the nucleus. Bohr and Wheeler gave a quantitative explanation of the fission process in their classic paper of 1939. It is postulated that nuclear attractive forces tend to keep the nucleus in stable state akin to the surface tension to maintain liquid drop in a stable form resisting

distortion. For a drop of liquid to be broken into two smaller drops or for a nucleus to undergo fission, there must be a considerable distortion which will only be possible if additional energy is available. After absorbing a thermal neutron,  $^{235}\text{U}$  forms a compound nucleus and the binding energy gained is available to the CN as excitation energy. This  $E^*$  is the driving force to cause distortion of nucleus. Fission is viewed as a continuous evolution of nuclear shape starting from nearly spherical compound nucleus to two well separated fragments. Considering the nucleus as a uniformly charged sphere, the potential energy associated with the nuclear deformation can be calculated. The binding energy of the nucleus based on LDM is calculated as the sum of volume, Coulomb, surface, asymmetric and pairing energies.

This model is useful to explain the existence of fission barrier, energy release and other features. However, near constancy of the barrier height for actinides, asymmetric mass division, existence of fission isomers etc. could not be addressed by this model. By superimposing deformation dependent nuclear shell and nucleon pairing energy on LDM potential, Strutinsky calculated the potential energy as a function of deformation. He showed that fission barriers for actinides are double humped as shown in Fig. 1.2. A nucleus encounters two barriers and two valleys before it reaches scission point to undergo fission. For isotopes of elements with  $Z = 92$  to  $94$ , both the barriers having comparable heights. If a nucleus is trapped between the two barriers of comparable heights, then the nucleus have a finite life time before it tunnels through one of the barriers. These nuclear states are called “fission isomers” or “shape isomers”. If the isomer tunnels through the second barrier, it undergoes fission known as “isomeric fission” (IF). On the other hand if the excited nucleus tunnels first barrier and reaches ground state, then it is called  $\gamma$  deexcitation. If the nucleus tunnels through both barriers from its ground state and undergoes fission, it is called “spontaneous fission” (SF). SF is a decay process from ground state and IF can be observed only in the induced reactions.



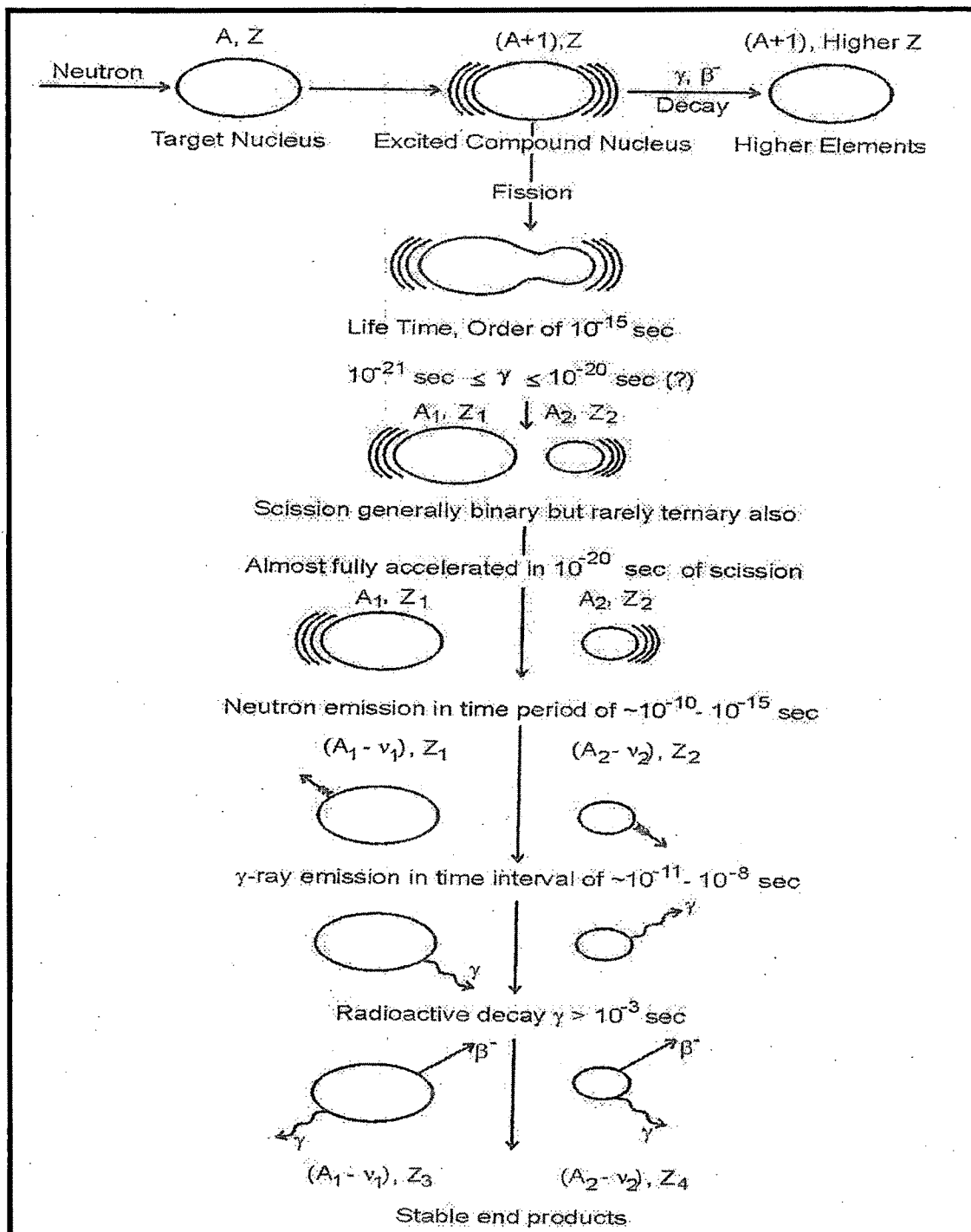


**Fig. 1.1 Schematic diagram of fission process**

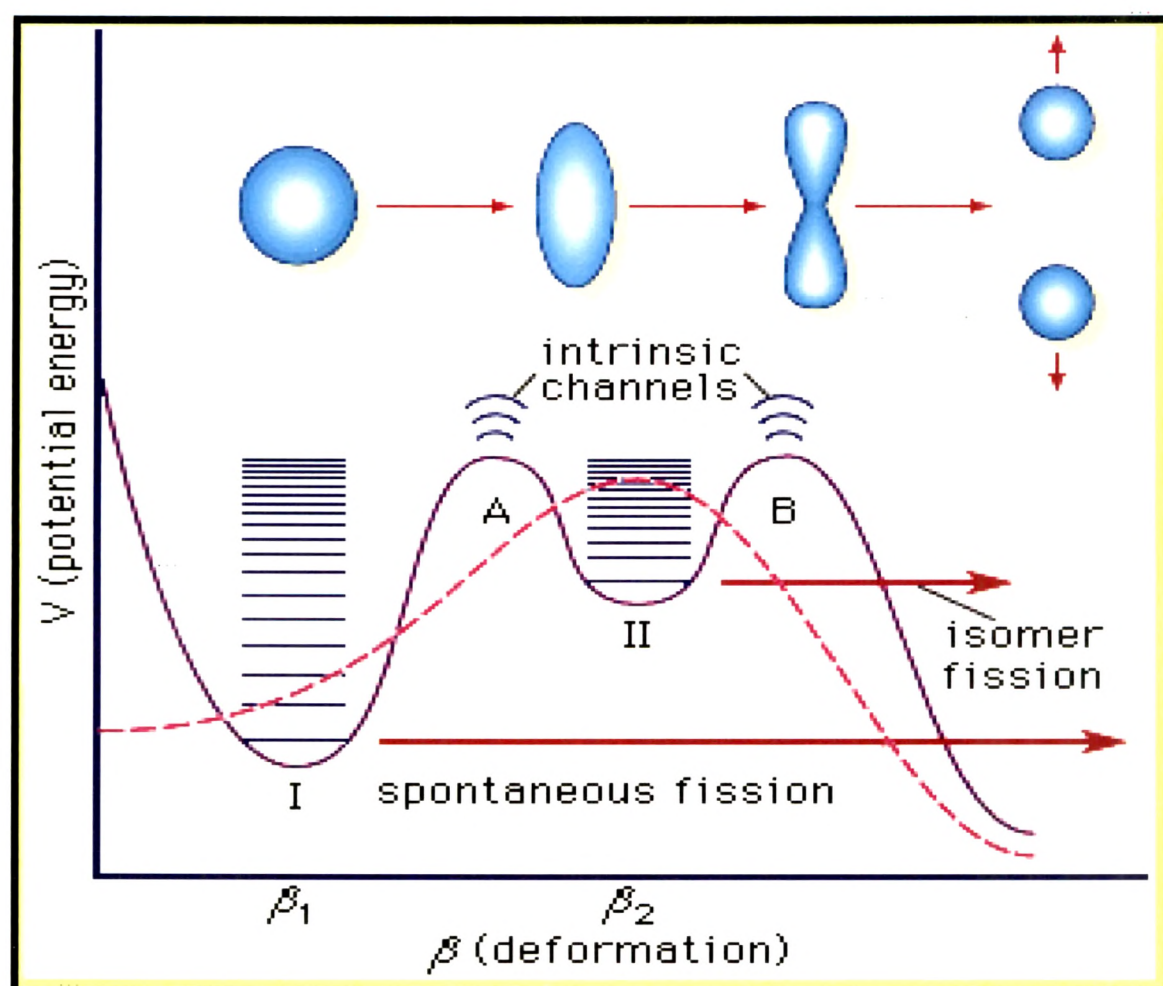


Fig. 1.2 Potential energy diagram showing the double-humped fission barrier

### 1.2.1.3 Types of Fission Yields

The mass and charge of the products formed in the fission are in the range of  $A=70-160$  and  $Z=30-65$ , having a wide range in the yields (0.0001 % to 7 %), as shown in Fig. 1.3. The nature of the yield distribution of the products is predominantly asymmetric with maximum yield of about 7 %. The peaks are around  $A=90-100$  in the lighter mass region and around  $A=134-144$  in the heavier mass region. An interestingly the yield around  $A=117$  corresponding to the symmetric mass division is low (0.01%). The two peaks and the valley are the features of the mass distribution in the low energy fission. There are about 400 fission products with half-lives ranging from less than a second to tens of years. The fission products are neutron rich compared to the stable nuclides of the same mass number and undergo  $\beta$  decay. The different types of fission yields are defined as follows.

- a) **Independent Yield:** Percentage of yield of any fission product formed from the fissioning nuclei.
- b) **Cumulative Yield:** Summation of the independent yield percentage of all fission products up to the nuclide of interest in a given mass chain formed from the fissioning nuclei.
- c) **Mass Chain Yield:** Summation of the independent yield percentage of all fission products in a given mass chain formed from the fissioning nuclei.
- d) **Charge Chain Yield:** Summation of the independent yield percentage of all fission products for different masses of an element formed from the fissioning nuclei.

A target of the fissile isotope, e.g.,  $^{235}\text{U}$  is prepared on a suitable backing. It is irradiated in a reactor with a known neutron flux ( $\Phi$ ). The products formed are absorbed in a catcher such as aluminum foil. The activities of the individual products are measured either by direct gamma ray spectrometry or by measuring the activities of the radiochemically separated products from the catcher foils. The activity of a given mass ( $A$ ) is related to fission yield ( $Y$ ) by eq.1

$$A_i = N\sigma\Phi Y(1 - e^{-\lambda t}) \quad (1)$$

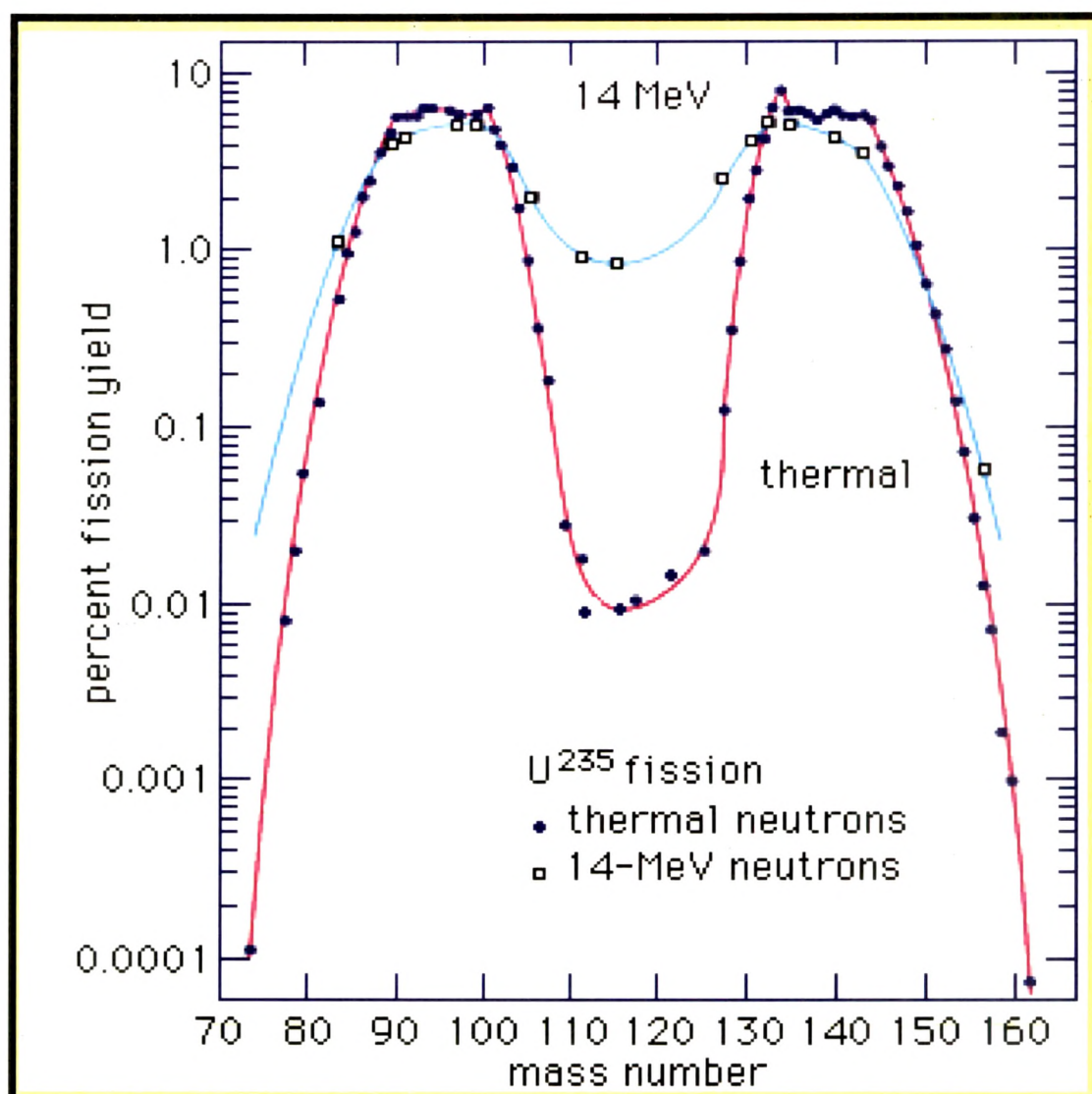


Fig. 1.3 Fission yield as a function of mass number for thermal and 14 MeV neutron-induced fission of  $^{235}\text{U}$ .

Where,  $A_i$  is the zero time activity without abundance and efficiency,  $N$  is the number of fissile atoms in the target,  $\sigma$  is the fission cross-section,  $\Phi$  is the neutron flux,  $\lambda$  is the decay constant of the product,  $t$  is the irradiation time.

The yields of many masses have to be determined to obtain the mass yield curve. The yields are plotted as a function of mass of the product and the area under the curve is summed and normalized to 200 %. From the normalized curve, yields of the products are obtained that could not be determined experimentally. More than 70% of the yields are concentrated in two groups around  $A = 90-100$  and  $A = 134-140$ . In the low energy fission, mass distribution is predominantly asymmetric and heavy peak position is around mass 139-140 which is attributed to the influence of double magic shell configuration (deformed shell). In the case of neutron-induced fission of  $^{239}\text{Pu}$ , the heavy peak position remains same as that in  $^{235}\text{U}(n_{th}, f)$  where as the light peak gets shifted to right by about 3 mass units.

The width of the distribution of the two peaks is around 12-14 mass units. The peak to valley ratio for  $^{235}\text{U}(n_{th}, f)$  is about 600 and decreases with increasing mass of the fissioning nucleus. When the kinetic energy of the projectile ( $n, p, \alpha \dots$ ) is increased, the yields in the valley start increasing and at around  $E = 100$  MeV, mass yield distribution is a single peaked i.e. symmetric division becomes more probable. In a given mass chain there are many isobars. Each isobar is formed with a definite yield in the fission process, known as independent yield. Each isobar is having different charge or atomic number. The distribution of independent yields of different charges for a given isobaric chain is called charge dispersion or charge distribution. The charge distribution in low energy fission is characterized by most probable mass ( $Z_p$ ) and width of the distribution ( $\sigma_z$ ) and the independent yield of each charge is represented by eq. 2 as follows

$$I.Y = \int_{Z-0.5}^{Z+0.5} \frac{1}{\sqrt{2\pi\sigma_z^2}} \exp\left[-\frac{(Z-Z_p)^2}{2\sigma_z^2}\right] dz \quad (2)$$

By measuring more than two independent yields,  $Z_p$  and  $\sigma_z$  can uniquely be determined. The radiochemical separations are very useful in charge distributions investigations.

### 1.2.2 Neutron Activation method – A tool for Neutron Cross-section Measurement

Neutron Activation Analysis (NAA) is a quantitative and qualitative method of high efficiency for the precise determination of a number of main components and trace elements in different types of samples [13]. NAA, based on the nuclear reaction between neutrons and target nuclei, is a useful method for the simultaneous determination of about 25-30 major, minor and trace elements of geological, environmental, biological samples in ppb-ppm range without or with chemical separation.

#### 1.2.2.1 Principle of Neutron Activation Analysis (NAA)

In NAA, samples are activated by neutrons. The product formed in neutron-induced reaction is often a radioisotope. Then the activated nucleus decays according to a characteristic half-life; some nuclides emit particles only, but most nuclides emit gamma-quanta, too, with specific energies. By measuring the radioactivity of the isotope formed, preferably with a high resolution germanium detector (e.g. HPGe), concentration of the isotope that underwent nuclear reaction is measured. Using the isotopic abundance, elemental concentration can be calculated. As the irradiated samples contain radionuclides of different half-lives, different isotopes can be determined at various time intervals.

#### 1.2.2.2 Kinetics of activation [14]

In the case of nuclear reactions induced by neutrons, the radioactivity of the examined isotope depends on the flux of the neutrons and the cross section of the given nuclear reaction. The cross section and the neutron flux highly depend on the energy of neutrons, and therefore the usual activation equation is:

$$R = N \int_0^{\infty} \sigma(E) \cdot \varphi(E) dE \quad (3)$$

where, N: number of interacting isotopes

$\sigma(E)$ : cross-section [in  $\text{cm}^2$ ] at neutron energy of E [in eV]

$\varphi(E)$ : neutron flux per unit of energy interval [in  $\text{cm}^{-2} \text{s}^{-1} \text{eV}^{-1}$ ]

R: reaction rate

In nuclear reactors the integral in equation 3 is usually replaced by the sum of two integrals separating the thermal and epithermal regions, the lower limit of the epithermal component of a neutron spectrum most commonly is 0.55 eV:

$$R = N (\phi_{th} \cdot \sigma_{th} + \phi_e \cdot I_0) \quad (4)$$

where,  $\phi_{th}$ : conventional thermal neutron flux [in  $\text{cm}^2$ ]

$\sigma_{th}$ : effective thermal neutron cross-section [in  $\text{cm}^2$ ]

$\phi_e$ : conventional epithermal neutron flux [in  $\text{cm}^{-2} \text{s}^{-1} \text{eV}^{-1}$ ]

$I_0$ : resonance integral cross section (in epithermal region),  
for 1/E epithermal spectrum [in  $\text{cm}^2$ ]

#### 1.2.2.3 Advantages and Limitations of NAA [12]

The NAA technique has the advantageous properties like high sensitivity and selectivity, inherent accuracy and precision and low matrix effect in the estimation of many elements. The INAA (Instrumental NAA) technique is non-destructive, which helps in minimal sample handling. Both its inherent potential for accuracy and totally independent principle as a nuclear property based technique, which is not the case of many competing techniques, makes NAA as an invaluable reference technique. It has self-validation possibility e.g., an element has more than one isotope and one isotope has more than one characteristic gamma line, which forms the basis for a unique ability to verify analytical data.

NAA has some limitations as well. It needs a neutron source like nuclear reactor that is available at a few research centers. Determination of elements forming very short-lived, long-lived or only  $\beta^-$  emitting isotopes is difficult by conventional NAA. Determination of elements forming long-lived isotopes is time consuming. NAA is insensitive to the nature of chemical species present unless pre-irradiation separation is carried out. The conventional NAA is not preferred for certain elements like Si, P, Pb, B, Gd and low Z elements.

### 1.2.3 Role of Structural materials in reactor technology

The structural materials (e.g. Zr, Nb, Fe, Ni, Al...) represent the key for containment of nuclear fuel and fission products as well as reliable and thermodynamically efficient production of electrical energy from nuclear reactors. Similarly, high performance structural materials will be critical for the future success of proposed fusion energy reactors, which will subject the structures to unprecedented fluxes of high-energy neutrons along with intense thermo-mechanical stresses. Advanced materials can enable improved reactor performance via increased safety margins and design flexibility, in particular by providing increased strength, thermal creep resistance and superior corrosion and neutron radiation damage resistance. In many cases, a key strategy for designing high-performance radiation resistant materials is based on the introduction of a high, uniform density of nanoscale particles that simultaneously provide good high temperature strength and neutron radiation damage resistance.

## 1.3 Various types of Neutron sources

Neutrons are produced in nuclear reactions. Therefore, all neutron sources are made by exploiting various types of nuclear reactions induced by either by high energy charged ions or high energy electromagnetic radiation. A very brief description of different types of neutron sources is given below.

### 1.3.1 Neutrons from uranium fission - Nuclear Reactors

One of the most neutron sources is the fission reaction. The fission process is accompanied by the emission of the fast neutrons. Nuclear reactions utilizing the phenomenon of nuclear fission in uranium (mostly thermal neutron fission in  $^{235}\text{U}$  isotope) at present provide the most important and most intense source of neutrons.

Owing to the high neutron flux, experimental nuclear reactors operating in the maximum thermal power region of 100 kW - 10 MW with a maximum thermal neutron flux of  $10^{12}$ - $10^{14}$  neutrons  $\text{cm}^{-2} \text{s}^{-1}$  are the most efficient neutron sources for high sensitivity activation analysis induced by epithermal and thermal neutrons. The reason for the high sensitivity is that the cross section of neutron activation is high in the thermal region for the majority of the elements. There



is a wide distribution of neutron energy in a reactor and, therefore, interfering reactions must be considered. In order to take these reactions into account, the neutron spectrum in the channels of irradiation should be known exactly. e.g. if thermal neutron irradiations are required, the most thermalized channels should be chosen.

### 1.3.2 Radioactive ( $\alpha$ , n) sources

In the case of the most frequently used isotopic neutron sources, an alpha emitting radioactive material is mixed with beryllium and an ( $\alpha$ , n) reaction generates the neutrons. The different types of ( $\alpha$ , n) are given below in Table 1.1.

**Table 1.1 Isotopic Neutron Sources**

$\alpha$ -emitter	Half life	Neutrons $s^{-1} Ci^{-1}$ emitted	Average neutron energy [MeV]
$^{227}Ac$	22 y	$1.5 \times 10^7$	4
$^{226}Ra$	1620 y	$1.3 \times 10^7$	3.6
$^{239}Pu$	$2.4 \times 10^4$ y	$1.4 \times 10^7$	4.5
$^{210}Po$	138 d	$2.5 \times 10^6$	4.3

The spontaneous fission of some artificially produced transuranium isotopes can be applied as a small neutron source. E.g.  $^{252}Cf$  (half-life 2.6 y) undergoes fission, producing 3.76 neutrons of 1.5 MeV per event. One milligram of  $^{252}Cf$  emits  $2.28 \times 10^9$  neutrons per second. The major advantage is that the isotopic neutron sources can be made portable and generate a stable neutron flux. But, as the neutron flux is rather low in comparison to a nuclear reactor their use in NAA is limited to the determination of elements of high activation cross section which are present in major concentrations.

### 1.3.3 Accelerated charged particle based neutron sources

Two-body reactions are a convenient and powerful way to produce monoenergetic neutrons. These sources are preferred for the production of intense beams of mono-energetic neutrons. The projectiles include protons, deuterons, tritons,  $\alpha$  particles and some heavier nuclei accelerated in particle accelerators.

Accelerator-based neutron production by two-body reactions does not necessarily give a pure monoenergetic neutron beam. In many cases there will be a contamination with intrinsic neutron background (other neutron lines from the excitation of non-ground-state levels or neutrons from break-up reactions) and/or with structural and room background. In principle, such monoenergetic neutrons can be produced by two-body reactions. However, a practical source will not only produce these foreground (primary) neutrons, but also "background" neutrons, either from beam interactions in the accelerator and target structure or from interactions of the primary neutrons with the room structures (beam connected room background, in scattered neutrons). This background depends, of course, strongly on the "hardware" in use and not on the source reaction itself.

The yield of neutrons of the desired energy from an accelerator based monoenergetic source depends on, the charged particle beam intensity, the target thickness, the differential cross section of the reaction and the specific energy loss in the target material. The charged particle beam intensity is limited on the one hand by the capability of the accelerator, on the other hand by the maximum allowed heat load of the target because the power dissipated in the target depends on beam intensity and energy loss in the target. To achieve a high specific yield, it is necessary to have both a high neutron production cross-section and a small energy loss of the projectile in the target. The different types of accelerator based neutron source are given below in Table 1.2.

**Table 1.2 Neutron productions through charged particle accelerator**

<b>Reaction</b>	<b>Q- Value (MeV)</b>	<b>Mono- energetic neutron energy range (MeV)</b>
$^2\text{H}(\text{d}, \text{n})^3\text{He}$	3.270	2.45 – 7.71
$^3\text{H}(\text{d}, \text{n})^4\text{He}$	17.59	14.0 – 14.7
$^3\text{H}(\text{p}, \text{n})^3\text{He}$	-0.763	0.29 – 7.59
$^7\text{Li}(\text{p}, \text{n})^7\text{Be}$	-1.644	0.12 – 0.65

#### 1.3.4 Photo-neutron sources

These sources are prepared by utilizing  $(\gamma, \text{n})$  reaction on different targets. The targets, in general use, deuterium and  $^9\text{Be}$  isotope. The  $(\gamma, \text{n})$  reaction is endoergic. So, incident energy must exceed the threshold of the reaction for preparing these sources. The deuterium has the threshold of 2.226 MeV while  $^9\text{Be}$  has the threshold of 1.66 MeV. In principle, radioactive photo-neutron sources offer the possibility of obtaining mono-energetic neutrons. If radioactive nucleus emits only one gamma ray with energy above the threshold for the  $(\gamma, \text{n})$  reaction in either beryllium or deuterium, the neutrons emitted should all be of the same energy, except for a small spread in energy resulting from differences in the direction between the gamma ray and the emitted neutron.

#### 1.4 Solid State Nuclear Track Detector (SSNTD)

'SSNTD' stands for Solid State Nuclear Track Detection, one of the most fascinating nuclear particle detection techniques, developed to date [15]. It has been found to be equally useful in basic and applied research work, particularly for scientists, engineers, and technologists in the developing countries. Solid State Nuclear Track Detectors were formed with the cooling

down of the insulating solid matter in the space around us. They have always been in existence on our earth, moon and other solidified matter (such as meteorites) since their cooling down in the form of minerals (i.e. feldspars, quartz, micas, etc.) and glassy matter. However, they were "rediscovered" only about three decades ago. Three American scientists, namely: Fleischer, Price and Walker, pioneered most of the early work in this field. In the beginning, mostly natural substances such as minerals were used as solid state nuclear track detectors. However, with the passage of time many man-made materials were successfully developed for their use as track detectors. Fleischer and his colleagues, not only developed the technique, but also applied it in almost every branch of science. The last two decades or so, saw the development and successful applications of this extremely useful scientific tool all over the world. With the passage of time the technique of SSNTD (inspite of its simplicity) became a powerful scientific tool. Not only this technique system is simple, inexpensive, employs very little electronics, is portable but also it has found some unique applications in almost all scientific fields.

There are several types of these detectors including inorganic crystals, glasses and plastics. When a heavily ionizing charged particle passes through such insulating solids, it leaves a narrow trail of damage about 50 Å in diameter along its path. This is called 'Latent Track' as it cannot be seen with the naked eye. It is possible to view this latent track with an electron microscope. The exact nature of the physical and chemical changes occurring at the damage site depends on the charge ( $Z$ ) and velocity ( $\beta = v/c$ , where  $v$  is the particle velocity and  $c$  is the velocity of light) of the particle, on the chemical structure of the detector material and also on the environmental conditions like temperature and pressure. These latent tracks can be enlarged / developed so that they can be viewed under an optical microscope by etching with some chemicals such as sodium hydroxide and hydrofluoric acid.

#### **1.4.1 An application of solid state nuclear track detector in nuclear fission**

The most direct and simplest use of the detectors involves exposure of a target, say of a fission material like U in contact with the track detector, to a flux of neutrons or charged particles, and the resulting energetic reaction products (in this case fission fragments) leave their tracks on the detector [16]. The number of tracks, ( $T$ ), is proportional to the number of target atoms ( $n$ ), the flux ( $\phi$ ), the reaction cross section ( $\sigma$ ), and the time of irradiation ( $t$ ).



$$T \propto n\sigma\phi t \quad \text{or} \quad T = K_{\text{dry}} n\sigma\phi t$$

where  $K_{\text{dry}}$  = Registration Efficiency.

If  $W$  is the weight of the element in grams (g) containing a weight fraction,  $X$  of the fissile isotope of mass  $A$  and  $N$  is the Avogadro number, then the above equation becomes

$$T = K_{\text{dry}} \frac{W X N}{A} \sigma\phi t \quad (6)$$

Depending upon the need of the user, it is possible to measure any of the parameters, viz cross section ( $\sigma$ ), flux ( $\phi$ ) or amount ( $n$ ) of the target material, if  $K_{\text{dry}}$  is known. The charged particle track registration technique employing  $n$  SSNTDs is also used in many basic research studies in other fields of science.

In analytical applications, nuclear tracks are generally registered from thin sources of the samples in contact with the SSNTDs in  $2\pi$  geometry and the registration efficiency is close to unity.

### 1.5 A detailed literature survey related to the present work

The detail literature survey on fission yield measurements related to Th-U fuel cycle shows that [17-31] the exhaustive experimental work has been carried out in low energy neutron induced fission of actinides [17-31]. However, experimental nuclear data in medium to high-energy neutron induced fission of actinides which has immense importance for the design of advanced reactors and ADS are rare and very much limited [32, 33]. Most of the nuclear data in the neutron-induced fission of actinides from the compilation [32, 33] are based on average neutron spectrum of reactor. Therefore, there is strong need to measure fission products yields of Th, Pa and U in the medium energy region (5- 20 MeV) with mono-energetic neutrons apart from reactor neutrons. In the  $^{232}\text{Th}$ -  $^{233}\text{U}$  fuel cycle, the fissile nucleus  $^{233}\text{U}$  is generated by two successive  $\beta$ -decays after a neutron capture by the fertile nucleus  $^{232}\text{Th}$  as shown in fig. 1. Thus, the production of fissile nucleus  $^{233}\text{U}$  depends on the  $^{232}\text{Th}(n, \gamma)$  reaction cross-section. In ADS, the energy of neutrons is on higher side. Thus, the  $^{232}\text{Th}(n, \gamma)$  reaction cross-section at higher neutron energy has a strong impact on the performance and safety assessment for ADS.

The detail literature survey on  $^{232}\text{Th}(n,\gamma)$  reaction cross-section data indicates that there are many experimentally measured data are available for  $^{232}\text{Th}(n,\gamma)$  reaction over wide range of neutron energies from thermal to 2.73 MeV based on physical measurements [34-36] and activation technique [37-49]. Beyond 2.73 MeV, only one measured data of the  $^{232}\text{Th}(n,\gamma)$  reaction cross-section is available at 14.5 MeV [50] using the activation technique. At neutron energy higher than 6.44 MeV  $^{232}\text{Th}(n,2n)$  reaction starts and becomes the pre-dominant mode. Further, in the  $^{232}\text{Th}$ - $^{233}\text{U}$  fuel cycle as shown in Fig. 1, the production of  $^{233}\text{U}$  is controlled by the 26.967 days half-life  $^{233}\text{Pa}$  and thus the neutron induced fission/reaction and neutronics properties of the latter nucleus influence directly the inventory of the fissile material  $^{233}\text{U}$ . Thus knowledge on the neutron induced fission/reaction of  $^{233}\text{Pa}$  is essential for the design of AHWR and ADS. So far sufficient data of neutron-induced  $(n, \gamma)$  reaction cross-sections [51, 52] and  $(n, f)$  cross-sections [53-57] of  $^{233}\text{Pa}$  from direct and indirect measurements are available in the literature. From these data, it can be seen that  $^{233}\text{Pa}$  has a very low fission cross-section of  $<0.1$  b [58] for low energy (0.025 eV) neutrons due to its higher fission threshold. On the other hand, it has a sufficiently high neutron absorption cross-section of 39.5 b [58] to produce  $^{234}\text{Pa}$ , which can undergo fission by additional thermal neutron capture. A literature survey indicates that there is no data available for the neutron induced fission cross-section of  $^{234}\text{Pa}$  from direct or indirect measurements except the value of an upper limit quoted in Ref. [58]. This is because of the short half-life of 1.17 min for  $^{234}\text{Pa}^m$  and 6.7 h for  $^{234}\text{Pa}^g$ .

Zirconium is an important and major component of the structural materials used in traditional and advanced nuclear reactors, owing to its very low absorption cross-sections for thermal neutrons and resistance to corrosion. However, its cross-sections database especially for neutron threshold reactions is rather sparse [59, 60]. The International Atomic Energy Agency-Exchange Format (IAEA-EXFOR) database [61] shows significant discrepancy and gaps in the measured experimental data for many neutron threshold reactions. It also indicates that there has been no neutron capture  $(n,\gamma)$  reaction cross-section data available beyond the neutron energy of 2 MeV for many zirconium isotopes. Further, literature survey based on IAEA-EXFOR database shows that most of the thermal neutron activation cross-section measurements for zirconium isotopes were made in reactors with neutron spectra and thus was not precise for thermal neutrons.

### 1.6 Objective of the present thesis:

In view of the above discussions and explanations about the requirements of accurate and precise nuclear data to develop advanced nuclear systems, the main objectives of the present thesis are the following:

- (1). Fission products yield measurements in the fast neutron-induced fission of  $^{232}\text{Th}$  using recoil catcher and gamma-ray spectrometry technique. The experiment was carried out at the BARC-TIFR Pelletron Facility at Mumbai, India. The average neutrons (i. e quassi mono-energetic neutrons) were produced by  $^7\text{Li}(p, n)$  reaction at various proton energies.
- (2). Measurements of neutron capture cross-section, namely, for  $^{232}\text{Th}(n, \gamma)$  and  $^{232}\text{Th}(n, 2n)$  reactions at various neutron energies. This experiment was also performed using the BARC-TIFR Pelletron Facility at Mumbai, India using the proton beam at various energies.
- (3). Determination of  $^{233}\text{Pa}(2n_{\text{th}}, f)$  fission cross-section using the solid state nuclear track detector technique. The neutron irradiation of the thorium target to produce  $^{233}\text{Pa}$  has been carried out using the APSARA reactor at BARC, Mumbai, India
- (4). Neutron-induced reaction cross-section measurement of certain structural materials, such as Zr isotopes has been done at APSARA reactor, Purnima Neutron Generator at BARC and at BARC-TIFR Pelletron facility, Mumbai, India.
- (5). The above measurements of neutron-induced reactions and fission cross-section data have been compiled into IAEA-EXFOR data base. In addition to these, the Indian experimentally measured nuclear physics data from various Indian laboratories and institutions have also been compiled into IAEA-EXFOR database as per NDS, IAEA guideline and requirements.

## 1.7 Content of the present thesis

The results of this work have been incorporated in thesis in the following eight chapters.

### Chapter – 1:

This chapter deals with the introduction of the topic of the present thesis along with the objectives drawn there from. The detailed literature survey and the objective of the thesis have been discussed at the end of the chapter.

### Chapter – 2:

Chapter 2 contains the brief description of AHWR and ADS systems in connection with Th-U fuel cycle in Indian perspective.

### Chapter – 3:

The neutron-induced fission yield measurements of  $^{232}\text{Th}$  at various neutron energies are included in chapter 3. The experimentally measured fission yields have been compared with available literature data.

### Chapter – 4:

This chapter mentions the neutron capture cross-section measurements of  $^{232}\text{Th}(n, \gamma)$  and  $^{232}\text{Th}(n, 2n)$  reactions at various neutron energies. The details of the neutron spectra generated from  $^7\text{Li}(p, n)$  reaction has also been discussed. The theoretical nuclear model based calculation for the experimentally measured data has been performed with TALYS 1.2 code. Further, the measured data has also been compared with latest available nuclear data libraries from ENDF-B/VII, JEND 4.0 and JEFF-3.2.

### Chapter – 5:

The determination of  $^{233}\text{Pa}(2n_{\text{th}}, f)$  fission cross-section by using the solid state nuclear track technique has been covered in chapter 5. In this chapter, radiochemical separation of  $^{233}\text{Pa}$  from the irradiated  $^{232}\text{Th}$  target has been given in detail. Further, theoretical calculation of  $^{233}\text{Pa}(2n_{\text{th}}, f)$  cross-section using nuclear model based code TALYS 1.2 has also been included in this chapter.



**Chapter – 6:**

The measurement of neutron-induced reaction cross-section for the Zr isotopes at different neutron energies is given chapter 6. Further, the comparison of the measured data with TALYS 1.2 and evaluated nuclear data libraries (ENDF-B/VII, JEND 4.0 and JEFF-3.2.) has been given in detail in this chapter.

**Chapter – 7:**

This chapter presents the compilation of the measured and published nuclear physics data from the present work in IAEA-EXFOR data base, NDS, IAEA. Further, the very brief introduction of IAEA-EXFOR data base has been covered in this chapter. In addition to these, the list of newly created EXFOR entries for the Indian nuclear physics data into IAEA-EXFOR database has also been included in this chapter.

**Chapter – 8:**

The summary and conclusions of present research work along with the future outlook has been given in chapter 8.

## References

- [1]. Analysis of Uranium Supply to 2050, IAEA 2001.
- [2]. Extending the global reach of nuclear energy through Thorium, Published by S. K. Malhotra, Head, Public Awareness Division, D.A.E, Govt. of. India, September 2008.
- [3]. S. S. Kapoor, *Pramana J. Phys.* 59, 941 (2002)
- [4]. R. K. Sinha, A. Kakodkar, *Nucl. Eng. Des.* 236, 683 (2006)
- [5]. C. Rubbia, et al., Conceptual Design of a Fast Neutron Operated High Power Energy Amplifier, CERN/AT/95-44 (ET) 1995
- [6]. C. D. Bowman, *Ann. Rev. Nucl. Part. Sci.* 48, 505 (1998)
- [7]. D. Saha and R. K. Sinha, Indian advanced nuclear reactors, Invited talk, Proceedings of Sixteenth Annual Conference of Indian Nuclear Society (INSAC-2005), Nov. 15-18, 2005, Mumbai
- [8]. R. K. Sinha and S. Banerjee, Nuclear energy to hydrogen, International Conference on Roadmap to Hydrogen Economy, INAE, Hyderabad, March 4-5, 2005
- [9]. S. Ganesan, *Pramana J. Phys.*, 68, 257 (2007).
- [10]. S. Ganesan, Proceedings of the International Topical Meeting on Advances in Reactor Physics and Mathematics and Computation into the Next Millennium, May 7-11, 2000, American Nuclear Society, Pittsburgh, Pennsylvania, USA.
- [11]. S. Ganesan, IANCAS Bulletin on "Physics in the Indian Nuclear Programme", Vol. IX, Nos. 1 & 2, January 2010.
- [12]. D. D. Sood, A. V. R. Reddy, N. Ramamoorthy, "Fundamentals of Radiochemistry" 3<sup>rd</sup> edition, 2007
- [13]. A. Vertes, S. Nagy, K. Suvegh, *Nuclear Methods in Mineralogy and Geology*, Plenum, New York and London (1998)

- [14]. D. Soete, R. Gijbels, J. Hoste, Neutron Activation Analysis, Wiley Interscience, New York, 1972
- [15]. R. H. Iyer. J. Chemical education, 49 (1972) 742
- [16]. P.C. Kalsi, A. Ramaswami, V. Manchanda, [www.barc.gov.in/publications/nl/2005/200506-2.pdf](http://www.barc.gov.in/publications/nl/2005/200506-2.pdf)
- [17]. R.J. Singh et al., Radiochimica. Acta **31**, 69 (1982).
- [18]. S.B.Manohar et al., Phys. Rev. **19**, 1827 (1979).
- [19]. S.A. Chitamber, H.C. Jain and M.V. Ramaniah, Radiochim. Acta **42**, 169 (1987).
- [20]. A. Ramaswami et al., Radiochim. Acta **30**, 11 (1982).
- [21]. R.H. Iyer et al., J. Inorg. Nucl. Chem. **25**, 465 (1963).
- [22]. M.N. Namboodiri, et al., J. Inorg. Nucl. Chem. **30**, 2305 (1968).
- [23]. H. Naik et al., Radiochim. Acta **75**, 51 (1996).
- [24]. R.H. Iyer et al., Nucl. Sci. and Eng. **135**, 227 (2000).
- [25]. H. Naik et al., Nucl. Phys. A **612**, 143 (1997).
- [26]. H. Naik, R.J. Singh and R.H. Iyer, Eur. Phys. J. A **16**, 495 (2003).
- [27]. H.Naik, R.J. Singh and R.H. Iyer, J. Phys. G: Nucl. Part. Phys. **30**, 107 (2004)
- [28]. H. Naik, S.P. Dange and A.V.R. Reddy, Nucl. Phys. A **781**, 1 (2007)
- [29]. H.Naik, S.P. Dange, R.J. Singh,T. Datta, Nucl. Phys. A, **587**, 273 (1995)
- [30]. H. Naik, S.P. Dange, R.J. Singh, Phys. Rev. C **71**, 014304 (2005).
- [31]. H. Naiket al., Eur. Phys. J. A **31**, 195 (2007)
- [32]. T.R. England and B.F. Rider, "Evaluation and Compilation of Fission Products Yields," ENDF/BVI (1989)
- [33]. M. James and R. Mills, "Neutron induced Fission Products Yields," UKFY2 (1991)

- [34]. R. C. Little et al., Nucl. Sci. Eng., **79**, 175 (1981).
- [35]. A. Borella et al., Nucl. Sci. Eng., **152**, 1 (2006).
- [36]. G. Aerts et al., Phys. Rev. C **73**, 054610 (2006)
- [37]. H. Pomerance, Phys. Rev. **88**, 412 (1952).
- [38]. R. L. Macklin, N. H. Lazar and W. S. Lyon, Phys. Rev. **107**, 504 (1957).
- [39]. J.A. Miskelet al., Phys. Rev. **128**, 2717 (1962).
- [40]. D. C. Stupegia, B. Smith and K. Hamm, J. Inorg. Nucl. Chem. **25**, 627 (1963)
- [41]. M. C. Muxon, TRDWP/P-8, U.K. Atomic Energy Authority, Harwell (1963).
- [42]. L. Forman et al., Phys. Rev. Lett. **27**, 11 (1971).
- [43]. V.B. Chelnokov et al. USSR Obninsk Report Jaderno Fizicheskii Issledovanija-13  
P. 16 (Oct. 1972).
- [44]. M. Lindner, R. J. Nagle and J. H. Landrum, Nucl. Sci. Eng. **59**, 381 (1976).
- [45]. R. E. Chrienet al., Nucl. Sci. Eng. **72**, 202 (1979).
- [46]. G.T. Baldwin and G.F. Knoll, Nucl. Sci. Eng. **88**, 123 (1984).
- [47]. R. T. Jones, J. S. Merritt and A. Okazaki, Nucl. Sci. Eng. **93**, 171 (1986).
- [48]. K. Wisshak, F. Voss and F. Kappeler, Nucl. Sci. Eng. **137**, 183 (2001).
- [49]. D. Karamanis et al., Nucl. Sci. Eng. **139**, 282 (2001).
- [50]. J. L. Perkin, L. P. O'connor, R. F. Colemann, Proc. Phys. Soc. (London), **72**, 505  
(1958).
- [51]. J. Halperin et al., Nucl. Sci. Eng. **1**, 1 (1956)
- [52]. S. Boyer et al., Nucl. Phys. A **775**, 175 (2006)

- [53]. H.R. von Gunten, R.F. Buchanan, and K. Behringer, Nucl. Sci. Eng. **27**, 85 (1967)
- [54]. F. Toversson et al., Phys. Rev. Let. **88**, 062502-1 (2002).
- [55] F. Toversson et al., Nucl. Phys. A **733**, 3 (2004).
- [56]. M. Petit et al., Nucl. Phys. A **735**, 345 (2004)
- [57]. B.K. Nayak et al., Phys. Rev. C **78**, 061602 (2008).
- [58]. S.F. Mughabghab, M. Divadeenam and N.E. Holden, Neutron Resonance and Thermal Cross Sections, Vol I, Academic Press, New York (1981).
- [59]. V. McLANE, C. L. Dunford and P. F. Rose, "Neutron Cross-Sections," Vol. **2**, Academic Press, San Diego (1988)
- [60]. R. C. Ward, I. C. Gomes and D. L. Smith, "A survey of selected neutron activation reactions with short-lived products of importance to fusion reactor technology," Report IAEA- INDC (USA) - **106**, Vienna (1994).
- [61]. IAEA-EXFOR Database, at <http://www-nds.iaea.org/exfor>.